Hindawi Publishing Corporation
Mathematical Problems in Engineering
Volume 2012, Article ID 956191, 14 pages
doi:10.1155/2012/956191

*Research Article*

# A Novel Detection Scheme for EBPSK System

**Xianqing Chen and Lenan Wu**

*School of Information Science & Engineering, Southeast University, Sipailou 2, Nanjing 210096, China*

Correspondence should be addressed to Xianqing Chen, xqchen213@126.com

Received 5 September 2012; Revised 21 October 2012; Accepted 23 October 2012

Academic Editor: Wuquan Li



We introduce the extended binary phase shift keying (EBPSK) communication system which is different from traditional communication systems by using a special impacting filter (SIF) for demodulation. The joint detection technique is applied at the demodulator side in order to improve the performance of the system under intersymbol interference (ISI). The main advantage of the joint detection technique, when compared to conventional threshold approaches, lies in its ability to use the amplitude and the correlation between neighboring bits, thus significantly improving performance, with low complexity. Moreover, we concentrate not only on increasing the bit rate of the system, but also on designing a bandwidth efficient communication system. Simulation results show that this new approach significantly outperforms the conventional method of using threshold decision by from 3.5 to 5 dB. The new system also occupies a narrower bandwidth. So joint detection is an effective method for EBPSK demodulation under ISI.

## 1. Introduction

In wireless communications systems, efficient use of the available spectrum is one of the most critical design issues. Therefore, modern communications systems must evolve to work as closely as possible to capacity, in order to achieve the required binary rates. In wireless sensor networks [1], sensor nodes are typically powered by batteries with a limited lifetime, and even though energy-scavenging mechanisms can be adopted to recharge batteries through solar panels and piezoelectric or acoustic transducers, energy is still a limited resource and must be used judiciously. Efficient use of the sensor node battery's energy is therefore an important aspect of sensor networks. For these reasons, many researchers have paid attention to this problem and proposed many energy management schemes [2–4]. In order to satisfy the ever increasing demand for such systems, an extended binary phase shift keying (EBPSK) system with very high spectra efficiency is introduced in [5]. A special impact filter (SIF) [6], which can produce high impact at the phase jumping point, with narrow bandwidth,

and great improvement in output signal noise ratio (SNR), was applied at the demodulator side. Therefore, following a simple amplitude detector would perform the demodulation of EBPSK signals. However, it is difficult to detect the signals of SIF output via a threshold decision under intersymbol interference (ISI), and the performance becomes worse [7]. ISI elimination in a communications system is a very important and difficult problem. Usually, the system which has been interfered with will have a very poor bit error rate (BER) performance. Therefore, many researchers are proposing some new complicated methods to deal with ISI [8–10].

Traditionally, channel equalization is used to eliminate ISI, which is a major issue in digital communications. Several detection procedures have been proposed to address this problem, each with varying degrees of success, including the optimal solution based on maximum likelihood sequence estimation (MLSE) [11] and the machine learning technique [12, 13], which can be used to approximate MLSE decisions at a lower computational cost. However, we need to send a training sequence, which will increase the computational cost with the length of sequence increased [14].

On the other hand, as opposed to traditional communication systems, an EBPSK system with the SIF at the demodulator side converts the phase changing to amplitude impacting. If the bit duration is short or a narrowband band-pass filter (NBPF) is added to achieve a bandwidth efficient transmission and suppress the interference to other channels, then the neighboring symbols will interfere with the others [15, 16].

In this paper, we concentrate not only on increasing the bit rate of the system, but also on designing a bandwidth efficient communications system. Given the characteristics of EBPSK modulation techniques, we introduce a joint detection algorithm to eliminate the ISI resulting from the SIF and to achieve a bandwidth efficient transmission.

The rest of the paper is organized as follows. Section 2 is devoted to introducing an EBPSK communications system. We also describe the generation of ISI and the threshold decision of amplitude. We present the receiver scheme with joint detection in Section 3. In Section 4, we include illustrative experiments to compare the performance of the proposed detectors. Section 5 includes our conclusions along with some final comments.

## 2. EBPSK Communication System

### 2.1. EBPSK Modulation

In this section, we will give a brief introduction of EBPSK modulation. EBPSK modulation is defined as follows:

$$f_0(t) = A\sin\omega_c t, \quad 0 \le t < T,$$
$$f_1(t) = \begin{cases} -B\sin\omega_c t, & 0 \le t < \tau, \\ A\sin(\omega_c t), & \tau \le t < T, \end{cases} \tag{2.1}$$

where $f_0$ and $f_1$ are modulation waveforms corresponding to bit "0" and bit "1," respectively, $T = 2\pi N/\omega_c$ is the bit duration, $\tau = 2\pi K/\omega_c$ is the phase modulation duration, and $\theta$ is the modulating angle. $A$ and $B$ are the amplitude of bit duration and phase modulation duration, respectively. Obviously, if $\tau = T$ and $\theta = \pi$, (2.1) degenerates to the classical binary

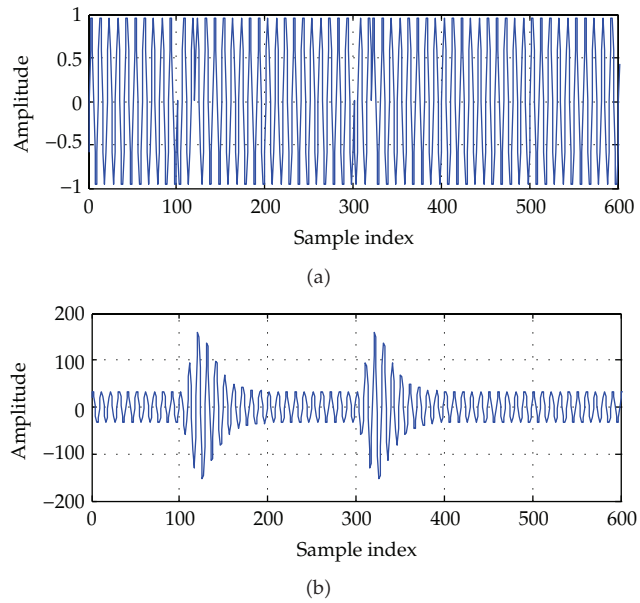


**Figure 1:** EBPSK modulation with $N = 10$, $\theta = \pi$, $K = 2$, $A = B = 1$ in (a) and SIF output in (b). The transmitted symbol sequence is $[0, 1, 0, 1, 0, 0]$.

phase shift keying (BPSK) modulation. As an example, Figure 1(a) is the waveform of EBPSK modulation and Figure 1(b) is the waveform of SIF output.

## 2.2. SIF and Demodulation

The waveforms of EBPSK modulation corresponding to "0" and "1" have very tiny differences. If we use the matched filter to demodulate, it has even high demand on input SNR. In order to improve the efficiency of the EBPSK signal as much as possible, the SIF method must be sought [17]. Figure 2 shows the amplitude-frequency response and phase-frequency response of the SIF. With one pair of conjugate zero poles, it reveals narrow notch-frequency-selecting performance near the center frequency.

The SIF with narrow bandwidth can produce high impact at the phase jumping point of EBPSK modulation waveform, with great improvement in output SNR. Obviously, following a simple amplitude detector would perform the demodulation of EBPSK signals, because of the existence of high impulse in coded 1s. Therefore, a direct threshold detector, which is the simple demodulation technique, can be used in the receiver.

Reference [18] gives the result which indicates we can get the optimal threshold if the symbols only interfere with additive white gaussian noise (AWGN). The threshold can be obtained as follows:

$$u_T = \frac{1}{2}\left( A_1 + A_0 + \frac{2\sigma^2}{A_0 - A_1} \ln \sqrt{\frac{A_0}{A_1}} \right), \tag{2.2}$$

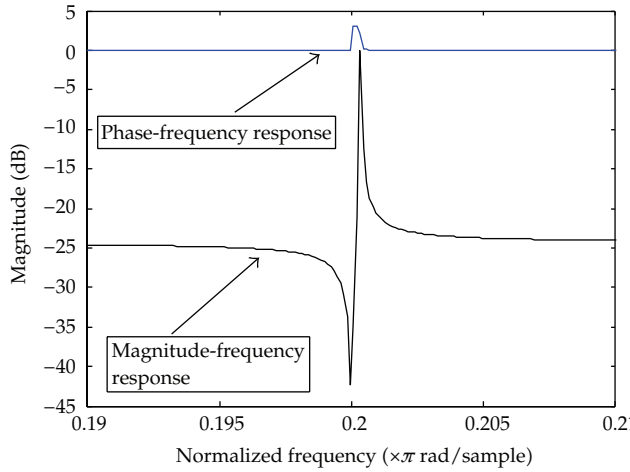


**Figure 2:** Amplitude-frequency response and phase-frequency response of the SIF with one pair of conjugate zero pole.

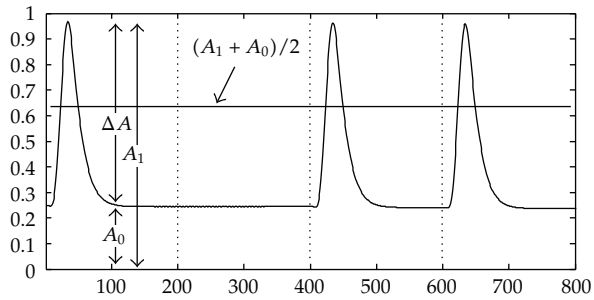


**Figure 3:** The threshold decision.

where $\sigma^2$ is the noise variance and $A_0$ and $A_1$ are the maximum amplitudes of the filter output corresponding to codes "0" and "1," respectively.

Figure 3 shows the envelope of the symbols where $\sigma^2 = 0$. Now, it is necessary to determine the value of $A_0$ and $A_1$. According to [6], the value of $A_0$ can be obtained through the following equation:

$$A_0 = A \cdot |H(\omega_c)| = \sqrt{\frac{2E_b}{T}} \cdot |H(\omega_c)|,$$
$$A_1 = A_0 + \Delta A. \tag{2.3}$$

On the premise of the existence of SIF, the value of $\Delta A$ has been deduced through the following results [18].

Assuming the transfer function of the impacting filter can be written as follows:

$$H(s) = \frac{A\prod (s - z_i)^{n_i}}{\prod_{i=1}^{m}(s - p_i)}, \tag{2.4}$$

then the transient response of the system can be calculated using the following [19]:

$$\begin{aligned} y(t) = & \sum_{i=1}^{m} \frac{-2A\omega\prod_{j=1}^{n}(p_i - z_j)^{n_j}}{(p_i^2 + \omega^2)\prod_{j=1, i\neq j}^{m}(p_i - p_j)} e^{p_i t}\varepsilon(t) \\ & + \sum_{i=1}^{m} \frac{2A\omega\prod_{j=1}^{n}(p_i - z_j)^{n_j}}{(p_i^2 + \omega^2)\prod_{j=1, i\neq j}^{m}(p_i - p_j)} e^{p_i(t-\tau)}\varepsilon(t-\tau) \\ & + \frac{-2A\prod_{i=1}^{n}(z_i^2 + \omega^2)^{n_i/2}}{\prod_{i=1}^{m}(p_i^2 + \omega^2)^{1/2}} \cdot \sin\left(\omega t - \sum_{i=1}^{m}\varphi_i + \sum_{i=1}^{n} n_i\phi_i\right)[\varepsilon(t) - \varepsilon(t-\tau)], \end{aligned} \tag{2.5}$$

where $\varphi_i$ and $\phi_i$ are the phase angles of pole and zero points, respectively. Therefore, the value of $\Delta A$ is equal to the maximum of (2.5).

However, when the symbol interferes with the neighboring symbols, it becomes difficult to detect the received symbols that we will analyze in the next subsection.

### 2.3. ISI and Threshold Decision

Communication channels introduce linear and nonlinear distortions, and in most cases of interest, they cannot be considered to be devoid of memory. ISI, mainly a consequence of multipath in wireless channels, accounts for the linear distortion. Unlike traditional communication systems, in this paper we will discuss two cases of ISI generation in EBPSK communication systems. Because of the characteristics of EBPSK modulation, in order to increase the bit rate, the bit duration $N$ becomes short, and so the signals of the SIF output will interfere with the others. On the other hand, most transmission systems have band limitations imposed by either the natural bandwidth of the transmission medium or by regulatory conditions. If a narrowband band-pass filter (NBPF) is added at the transmitting end of the communication system to achieve a bandwidth-efficient transmission, the symbols are also interfered with.

It is very difficult to detect the received symbols via a conventional threshold decision (CTD) when the symbols have interfered with the others, because the envelope of SIF output fluctuates considerably, as is shown in Figure 4. If we use a threshold decision, it is difficult to get the optimal threshold. However, the method which is referred to as an adaptive threshold may be considered. We could use dynamic threshold to adapt the envelope fluctuations; the threshold becomes high when the value of $A_1$ increases, and vice versa. However, even then we cannot ensure the correctness of the decision, because the value of $\Delta A$ changes considerably, as is shown in Part A of Figure 4. Therefore, this is not the proper methodology for EBPSK demodulation via threshold decision under ISI.

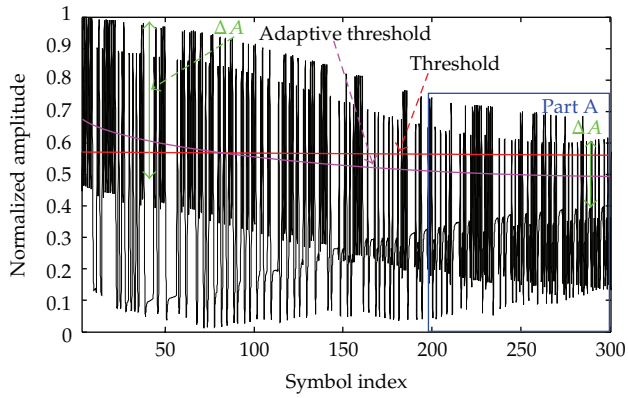


**Figure 4:** The signal envelope of SIF output under ISI.

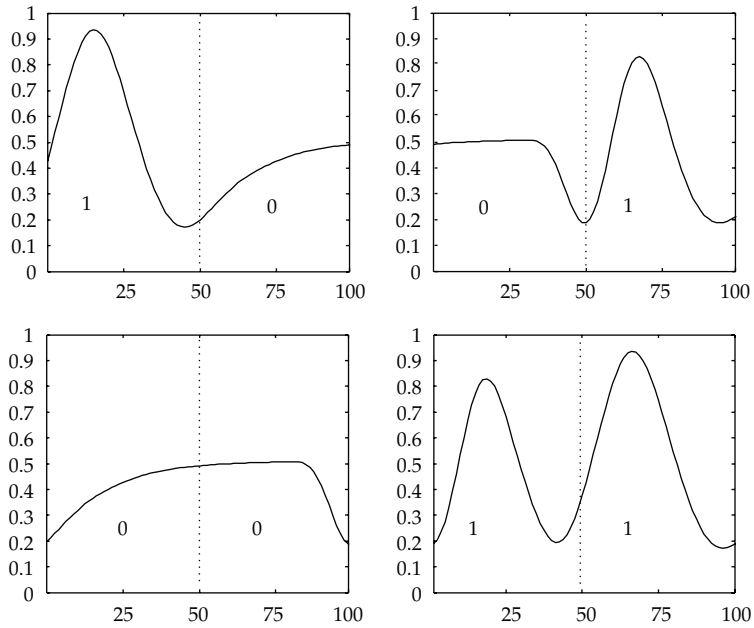


**Figure 5:** The signal template of $[0,0;0,1;1,0;1,1]$ under ISI.

## 3. Joint Detection

In the previous subsection, we have learned that it is difficult to detect the received symbols via threshold decision, and performance may worsen dramatically because of the ISI. In this section, we will introduce the detection based on the similarity of waveforms of SIF output and the correlation between symbols, which is referred to as joint detection (JD). The design approach is completely novel. We first divide two or more symbols into a group and then use the sampling points of the SIF output at intermediate frequency without downconversion to compute the correlation coefficient with the codebook, as shown in Figure 5.

Suppose $y(n)$ is the sequence of the SIF output which interfered with the AWGN and $x(n)$ is the noiseless template sequence. The similarity between them can be used to measure the error energy:

$$E^2 = \sum_{n=1}^{N} \left[x(n) - ky(n)\right]^2. \tag{3.1}$$

If $x(n)$ and $y(n)$ (or by multiplying factor $k$) are the same, then $E^2 = 0$. In general, the smaller the error energy $E^2$, the more similar the signals. In order to get the minimum value of $k$, let

$$\frac{\partial E^2}{\partial k} = 0. \tag{3.2}$$

Then

$$k = \frac{\sum_{n=1}^{N} x(n)y(n)}{\sum_{n=1}^{N} y^2(n)}. \tag{3.3}$$

Also, we can use the relative error to measure the similarity. Define relative error

$$\varepsilon^2 = \frac{E^2}{\sum_{n=1}^{N} x^2(n)}. \tag{3.4}$$

Then we can get

$$\varepsilon^2 = 1 - \frac{\left[\sum_{n=1}^{N} x(n)y(n)\right]^2}{\sum_{n=1}^{N} x^2(n) \cdot \sum_{n=1}^{N} y^2(n)} = 1 - \rho_{xy}^2, \tag{3.5}$$

where $E_{xy} = \sum_{n=1}^{N} x^2(n) \cdot \sum_{n=1}^{N} y^2(n)$ and $\rho_{xy}$ is the correlation coefficient. According to the Schwartz inequality $\left[\sum_{n=1}^{N} x(n)y(n)\right]^2 \leq \sum_{n=1}^{N} x^2(n) \cdot \sum_{n=1}^{N} y^2(n)$, we can get $|\rho_{xy}| \leq 1$. So if $\rho_{xy} = 1$, $\varepsilon^2 = 0$, then $x(n)$ and $y(n)$ have a perfect correlation, and $\rho_{xy}$ reflects the similarity between $x(n)$ and $y(n)$. Therefore, we can get the correlation coefficient $\rho_{xy}$ between the detection signal and template signal and make a preliminary decision as to whether or not $\rho_{xy} \geq \rho_T$, where $\rho_T$ is the correlation coefficient threshold, which will be discussed in detail later. The performance of detection will be affected due to noise levels. If we join the threshold $\rho_T$ and the threshold $u_T$ based on amplitude, which we deduced in the previous section as having the ability to detect the signal under ISI, we can make full use of the waveform and the amplitude of the signal. This detection is referred to as joint amplitude and waveforms detection (JAWD), which is described as follows.

Firstly, we divide two signal sequences of SIF output into one group and then compute the $\rho_{xy}$ between the received sequence $y(n)$ and the template sequence $x(n)$. If $\rho_{xy} \geq \rho_T$ means that $x(n)$ and $y(n)$ are similar, so we can get the detected symbols. If on the other hand $\rho_{xy} < \rho_T$, this means we cannot determine the values of the symbols. Finally, we use

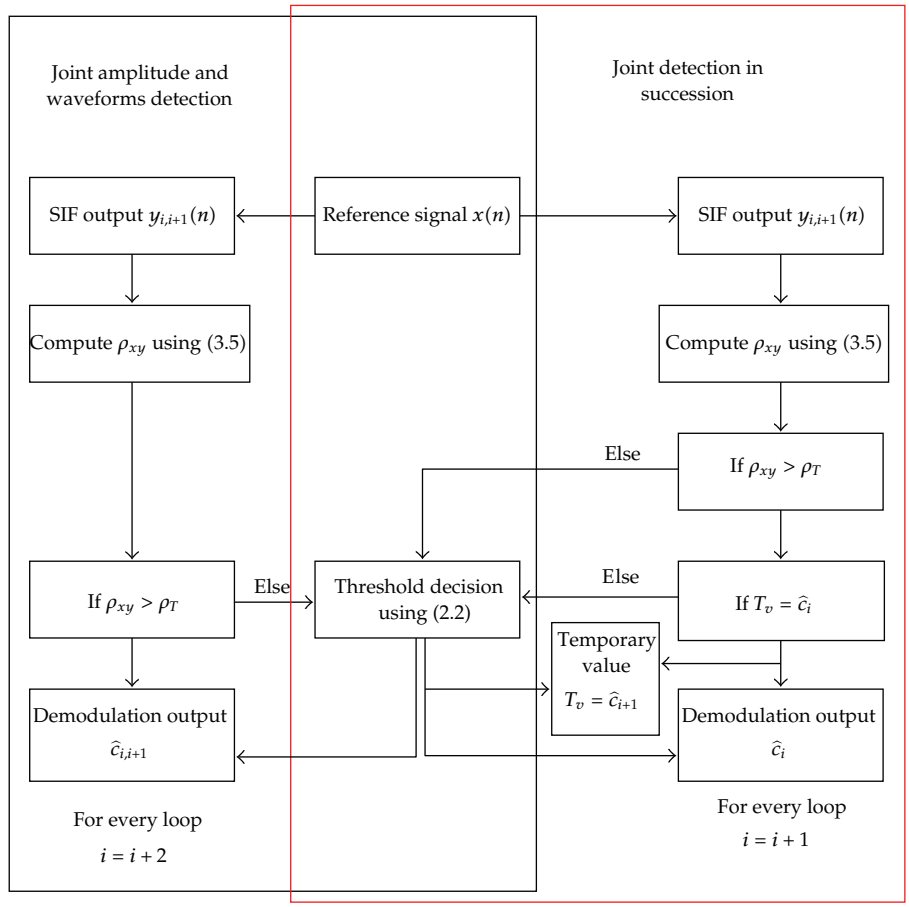


**Figure 6:** The procedure of JAWD and JDS.

the threshold $u_T$ to make a final decision and acquire the symbols. For every decision loop, we can get two symbols $c_{i,i+1}$.

In order to make full use of the correlation between neighboring symbols, another joint detection, which is referred to as joint detection in succession (JDS), is introduced. All procedures are similar to the JAWD, but for every loop, we only get one symbol $c_i$. The other symbol $c_{i+1}$ is stored in the temporary variable $T_v$ for verification in the next loop. In the $i+1$th loop, if $T_v = c_i$, then we get the symbol $c_i$ and update $T_v$ with new $c_{i+1}$, or else we use the amplitude threshold to make a decision and update the $T_v = c_{i+1}$. However, compared to the JAWD detection, the JDS only gets one symbol for every loop, and the temporary variable $T_v$ gives additional decisions. We can make full use of the correlation between every neighboring symbol. The procedures of JAWD and JDS are shown in Figure 6.

## 4. Simulation Results

In this section, we illustrate the performance of the proposed joint detection. Throughout our experiments, the reported BERs were computed using $10^5$ symbols, and we averaged

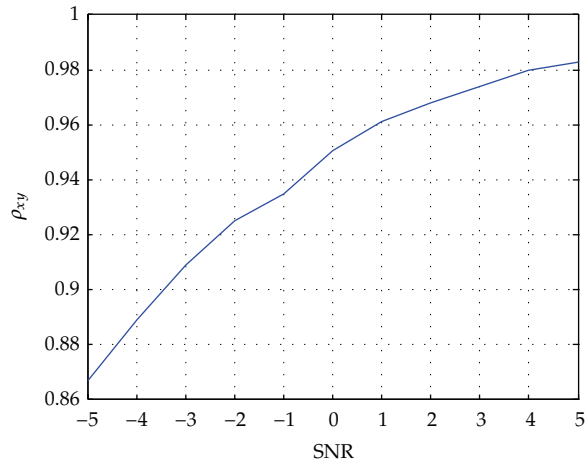


**Figure 7:** The value of $\rho_{xy}$ for different SNR with $N = 5$.

the results over 100 independent trials. During simulation, we chose $K = 2$, $A = B = 1$, $\theta = \pi$ as the parameters of EBPSK modulation. The whole system was simulated under MATLAB.

In what follows, we label the performance of the different detection techniques by JD for joint detection, JDS for joint detection in succession, CTD for conventional threshold detection, and JAWD and JAWD-3 for two and three joint symbols, respectively. The BER performance of the narrowband system is labeled with NB-JAWD, NB-JDS, and NB-TD.

### *4.1. Experiment 1: High Bit Rate System*

In this first experiment, we deal with the ISI generated by the short bit duration of the modulation parameter, which increases the bit rate of the system. We compare the JAWD with the JD, CTD, and artificial neural network (ANN) detection. Also, we will compare the performance of different joint detection methods with CTD and without ISI.

The JAWD we discussed in the previous section requires two thresholds; one is the conventional threshold $u_T$, and the other is the threshold of correlation coefficient $\rho_T$. The former can be obtained through (2.2), but the latter is a little hard to determine, because $\rho_{xy}$ decreases with decreases in the SNR, as is shown in Figure 7. Therefore, the $\rho_T$ would also change to adapt the $\rho_{xy}$. It is generally accepted that there is a strong correlation between $x(n)$ and $y(n)$ with $\rho_T > 0.85$. In Figure 7, we know that $\rho_T > 8.6$ with SNR $> -5$, so it meets our requirements. In order to enhance the decision of the correlation coefficient, we choose $\rho_T = 0.9$ with SNR $> -3$ and $\rho_T = 0.85$ with SNR $\leq -3$.

In Figure 8, we can appreciate that the decisions provided by the conventional threshold, ANN classification, JAWD, and JD are quite different. The performance of JAWD outperforms the other detection technique and is superior by 1 to 2 dB when compared with the ANN and JD, respectively. The CTD only uses the amplitude and omits the waveforms, and JD is the opposite. Therefore, the JAWD significantly reduces the BER, because it not only concentrates on the correlation between neighboring symbols and the waveform of the symbol, but also uses the signal amplitude for decision when the demodulation by $\rho_T$ failed.

We have shown that the JAWD technique is far superior to the CTD. In Figure 9, we compare the BER performance of different joint detections to the CTD method. We can

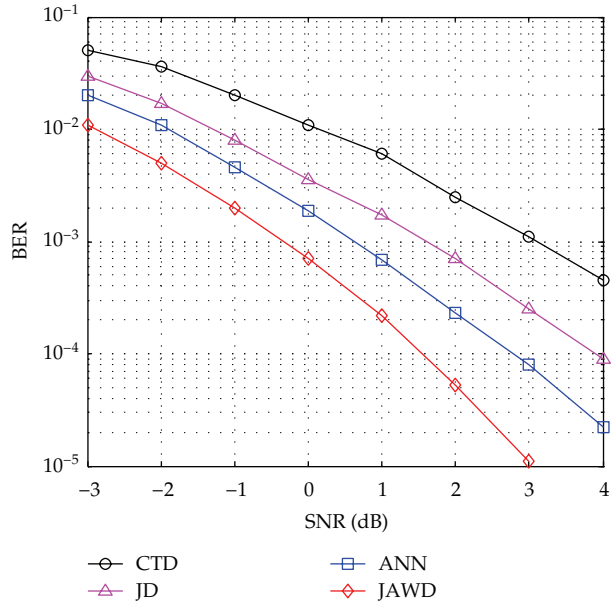


**Figure 8:** The performance comparison of different detection with $N = 5$.

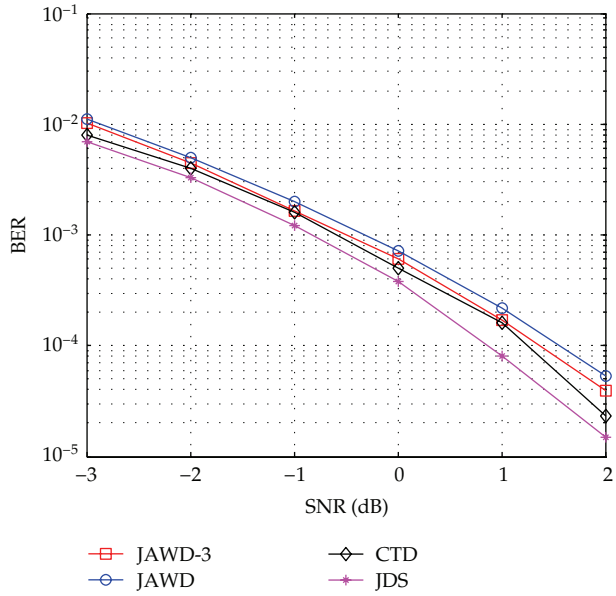


**Figure 9:** The performance of different joint detection techniques compared with CTD. We use $N = 5$ for JAWD, JAWD-3, and JDS; $N = 20$ for CTD.

appreciate that joint detection with two symbols performs similarly to three joint symbols. The performance of JDS is not only better than JD but also outperforms the threshold decision without ISI. This means that using CTD has difficulty allowing the system to perform to its fullest and that the JAWD or JDS techniques are a better choice.

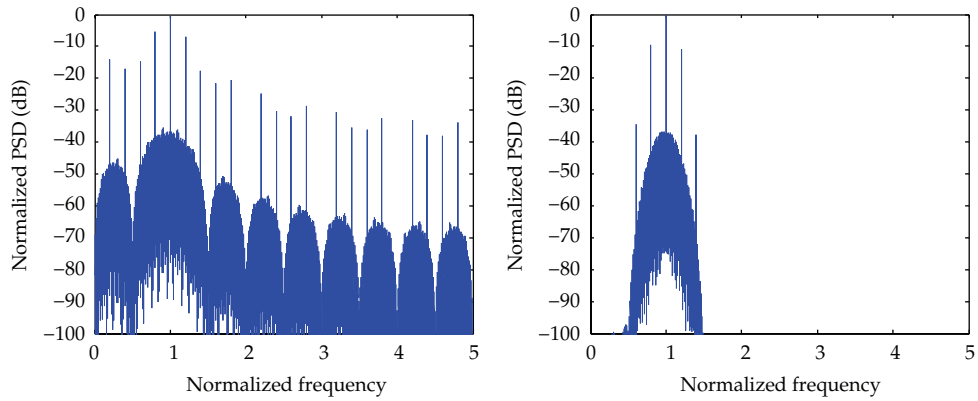


**Figure 10:** The power spectrum density of modulated signals and its filtered signals, respectively, in (a) and (b) for $K = 2$, $N = 5$.

From this first experiment, it is clear that we should use the JAWD or JDS for EBPSK demodulation while under ISI. Otherwise, we cannot get the desired BER performance. Also, we do not need to join three or even more symbols for detection, because the performances are almost identical, and the complexity is increased. Moreover, JDS is a little superior to JAWD and far superior to CTD, which even without ISI, because of the template variable, makes an additional decision for each symbol.

### *4.2. Experiment 2: Band-Limited System*

In the next experiment, we face a bandwidth efficient communication model, which is proposed via a narrowband band-pass filter at the transmitting end of the system. In order to reduce the ISI caused by the filter, we use the detection technique as described in the previous section.

The bandwidth of the linear phase NBPF is designed to be $[0.98N/T, 1.02N/T]$. Power spectrum density (PSD) of the modulated signals is plotted in Figure 10(a). When this signal is filtered by the NBPF, its corresponding spectrum is illustrated in Figure 10(b).

First of all, we should determine the $\rho_T$ by using JAWD. As described in the previous subsection, we have plotted the curve for $\rho_{xy}$ in Figure 11. We know that, if $\rho_T > 0.85$, then we can assume the signals are similar, and we can make a final decision, so as is shown in Figure 11, the $\rho_T > 0.85$ when the SNR $> -4$ dB. In order to improve the detection accuracy, we use $\rho_T = 0.9$ with SNR $> -1$ dB and $\rho_T = 0.85$ with SNR $\leq -1$.

The performance comparisons of different detection methods are presented in Figure 12. As is shown in Figure 12, both JAWD and JDS have the ability to significantly improve the quality of the receiver. For the JDS, the SNR gain over the JAWD is around 0.8 dB with BER $= 10^{-4}$. This demonstrates that significant performance gains can be obtained via the joint detection algorithm. The JDS outperforms the CTD by about 5 dB, when the BER $= 4 \times 10^{-3}$. This effect can be explained by noting that the joint detection algorithm makes full use of the relevance of the waveforms and amplitude of SIF output signals.

From these two experiments, a high bit rate communication system with narrow bandwidth can be obtained. In order to increase the bit rate, we can use short bit duration.

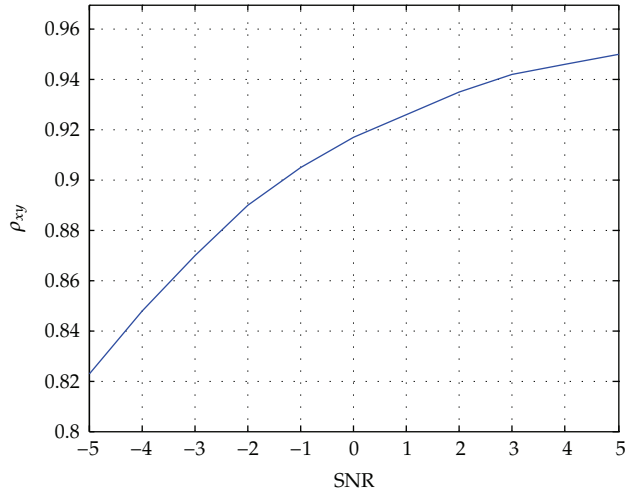


**Figure 11:** The value of $\rho$ for different SNR with bandwidth efficient system.

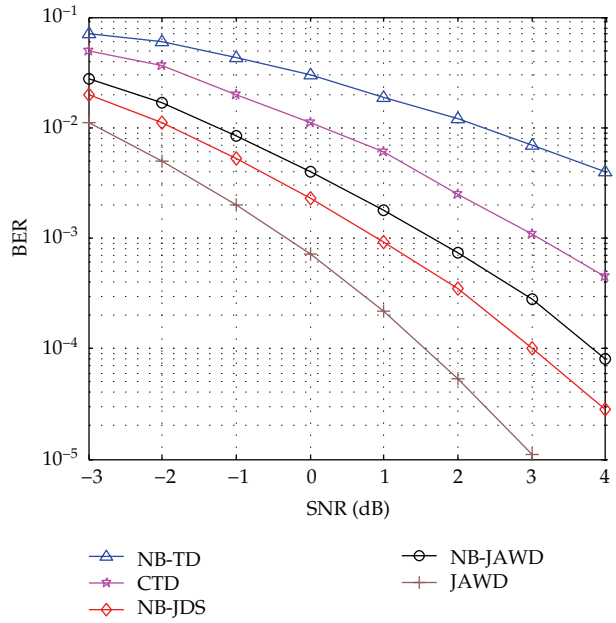


**Figure 12:** The performance comparisons of different detection techniques with bandwidth efficient systems and high rate systems.

The simulation shows that the BER performance is almost identical if we use JAWD or JDS, as compared to CTD with long bit duration. An NBPF added to the transmitting end can achieve a bandwidth efficient transmission by using JDS, which is only 1.5 dB inferior to the high bit rate, but a wide bandwidth system can be achieved by using JAWD.

## 5. Conclusions

In this paper, we introduced a novel solution for EBPSK communication systems based on joint detection technique. JDS and JAWD both use the amplitude and the correlation between two waveforms for detection, and the complexity of them is a little higher than CTD. We have shown that JDS and JAWD can significantly increase system performance under ISI and that the former outperforms the latter by more than 0.5 dB, with the cost of complexity.

A bandwidth efficient communication can work well without any channel equalizer, by using joint detection, which is different from traditional communication systems. Therefore, this system is always favorable, especially in a band-limited system, in which case the CTD may not work. Moreover, it is much simpler than an ANN demodulator and other equalizers, which need training before detection.

However, both the JDS and JAWD detectors are difficult to provide accurate posterior probability that can be exploited by a soft-input channel decoder to achieve capacity. The improvement of EBPSK performance by applying channel coding still has great potential. Therefore, future work will be focused on these problems.

## Acknowledgments

The authors thank all of the reviewers for their valuable comments, which have considerably helped in improving the overall quality of the work presented in the revised paper. This work is supported by the State 863 Project (2008AA01Z227), the National Natural Science Foundation of China (NSFC), under the Grant 61271204.

## References

[1] I. F. Akyildiz, S. u. Weilian, Y. Sankarasubramaniam, and E. Cayirci, "A survey on sensor networks," *IEEE Communications Magazine*, vol. 40, no. 8, pp. 102–114, 2002.

[2] S. Maheswararajah, S. Halgamuge, and M. Premaratne, "Energy efficient sensor scheduling with a mobile sink node for the target tracking application," *Sensors*, vol. 9, no. 2, pp. 696–716, 2009.

[3] C. Alippi, G. Anastasi, M. Di Francesco, and M. Roveri, "An adaptive sampling algorithm for effective energy management in wireless sensor networks with energy-hungry sensors," *IEEE Transactions on Instrumentation and Measurement*, vol. 59, pp. 335–344, 2010.

[4] G. Anastasi, M. Contib, M. Di Francescoa, A. Passarellab et al., "Energy conservation in wireless sensor networks: a survey," *Ad Hoc Networks*, vol. 7, no. 3, pp. 537–568, 2009.

[5] M. Feng and L. Wu, "Special non-linear filter and extension to Shannon's channel capacity," *Digital Signal Processing*, vol. 19, pp. 861–873, 2009.

[6] L. Wu and M. Feng, "On BER performance of EBPSK-MODEM in AWGN channel," *Sensors*, vol. 10, pp. 3824–3834, 2010.

[7] F. Man and W. Lenan, "Research on anti-fading performance of EBPSK system," in *Proceedings of 2nd International Symposium on Information Science and Engineering (ISISE '09)*, pp. 561–564, 2009.

[8] D. Shutin and B. H. Fleury, "Sparse variational Bayesian SAGE algorithm with application to the estimation of multipath wireless channels," *IEEE Transactions on Signal Processing*, vol. 59, no. 8, pp. 3609–3623, 2011.

[9] M. Miah, M. M. Rahman, T. K. Godder, and B. C Singh, "Performance analysis of an efficient wireless communication system in AWGN and slow fading channel," *Journal of Telecommunications*, vol. 5, no. 2, pp. 24–32, 2010.

[10] H. Zhao and J. Zhang, "Adaptively combined FIR and functional link artificial neural network equalizer for nonlinear communication channel," *IEEE Transactions on Neural Networks*, vol. 20, pp. 665–674, 2009.

[11] E. A. Lee and D. G. Messerschmitt, *Digital Communication*, Springer, 1994.

[12] F. Pérez-Cruz, A. Navia-Vázqueza, P. L. Alarcón-Dianab, A. Artés-Rodrígueza et al., "SVC-based equalizer for burst TDMA transmissions," *Signal Processing*, vol. 81, no. 8, pp. 1681–1693, 2001.

[13] F. Pérez-Cruz, J. J. Murillo-Fuentes, and S. Caro, "Nonlinear channel equalization with Gaussian processes for regression," *IEEE Transactions on Signal Processing*, vol. 56, no. 10, pp. 5283–5286, 2008.

[14] S. H. Kim, Y.-H. Sim, S.-W. Kim, C. Ahn, and D.-J. Kim, "Kalman-viterbi joint channel equalizer," Google Patents, 2009.

[15] Z. Mei, L. Wu, and S. Zhang, "Joint detection for a bandwidth efficient modulation method," in *Proceedings of the 9th international conference on Knowledge-Based Intelligent Information and Engineering Systems*, vol. 3683 of *Lecture Notes in Artificial Intelligence*, pp. 483–487, 2005.

[16] M. Feng and L. Wu, "Novel anti co-channel interference scheme for sensor networks," *Sensors*, vol. 10, pp. 3170–3179, 2010.

[17] M. Feng, L. Wu, and P. Gao, "From special analogous crystal filters to digital impacting filters," *Digital Signal Processing*, vol. 22, no. 4, pp. 690–696, 2012.

[18] F. Man, W.U. Lenan, J. Ding, and Q. I. Chenhao, "BER analysis and verification of EBPSK system in AWGN channel," *IEICE Transactions on Communications*, vol. 94, no. 3, pp. 806–809, 2011.

[19] N. Lu and L. Wu, "Transient response of filted PSK modulated signals," *Journal of Electrical & Electronic Education*, vol. 31, pp. 64–65, 2009.